SLAC-PUB-3045
January 1983
(I)

# MEASUREMENT AND SIMULATION OF THE DRIFT PULSES AND RESOLUTION IN THE MICRO-JET CHAMBER*

J. VA'VRA
*Stanford Linear Accelerator Center*
*Stanford University, Stanford, California 94305*

## ABSTRACT

We have tested a prototype of a micro-jet chamber [1], using both a nitrogen laser and a $10 GeV$ electron beam. The achieved resolution in the particle beam was $\sigma = 18 \mu m$ for a $1 mm$ impact parameter and $22 \mu m$ when averaging over the entire beam profile. The experimental results were compared to a Monte Carlo program which simulates the pulse shapes and resolution in drift chambers of any geometry. The main emphasis in our simulation analysis was to study various timing strategies for drift chambers in order to achieve the best possible timing resolution.

* Work supported by the Department of Energy, contract DE-AC03-76SF00515

Presented at the 1983 Wirechamber Conference, Vienna, Austria
February 15-18, 1983

# 1. INTRODUCTION

We have tested a possible solution for a vertex detector based on the micro-jet chamber concept [1]. The main reason for this choice was its relatively conservative design compared to more complex solutions based on the time expansion concept [10]. The following are the main features of the micro-jet chamber concept: a) high pressure ($\leq 6atm$), b) $1mm$ sample size, c) $7.8\mu m$ diameter sense wires, d) use of a $2-3ns$ rise-time amplifier, e) use of $TOF$ counter electronics to achieve the best possible timing resolution (timing resolution $\leq 0.5ns$ achieved), f) Lorentz angle of about $2^o$ at $15kG$, g) maximum drift time is less than $150ns$, h) finally, we prefer to use gases giving both a high gain and a relatively slow speed.

The chamber was extensively tested using both the nitrogen laser [2] and a $10GeV$ electron beam, both from the point-of-view of resolution and of pulse shape.

Presently our preferred gas is $90\% Ar + 10\% C_4H_{10}$. This gas has a rather large transverse diffusion; however, assuming that the longitudinal diffusion, which has not been measured to our knowledge, is half of the transverse diffusion, we expect to reach $\sim 15-20\mu m$ diffusion limit at $6atm$ and a $2mm$ impact parameter. Other gases are being tested. Table 1 shows the operating points and achieved measured results in some gases we have tried.

It appears that drift chambers in the future will operate in high density track environments. For the best double track separation, one needs to employ waveform digitizing electronics. However, this may not produce sufficiently good timing resolution. We have attempted to develop a complete Monte Carlo drift program [12] to study these problems in detail. The study was motivated by the very large cost and the complexity of existing waveform digitizing electronics. To simulate the drift pulse, one has to convolute several broadening contributions (see Appendix A):

1. Drift time distributions of the arrival of individual electrons at the anode wire.
2. Response of the avalanche due to the motion of positive ions.
3. Finally, we measure the response of the amplifier to an impulse charge and convolute it with all other contributions.

Once the waveform is generated, we define a threshold as, say $\sim 10\%$ of the average peak value, then find the crossing point of the waveform at the threshold. In this way, we can determine the expected resolution for a given timing strategy, such as leading edge timing with a single threshold, multiple threshold timing, centroid timing, et cetera.

## 2. RESULTS

Figure 1 shows the micro-jet chamber with its electronics. The chamber has six sense wires $10cm$ long, although only three were fully instrumented. The chamber was placed in a pressure vessel with two quartz windows to allow the nitrogen laser beam to enter the chamber. With a quartz lens of $f = 50cm$, we generated a vertical spot size of $250\mu m(FWHM)$, and in the vertical direction the electrons drifted toward the sense wires. The beam passed through the center of an anode-cathode gap. Figure 2b shows the $FND - 100$ diode pulse and the drift chamber pulse.

Figure 3 shows a comparison of the average laser generated drift pulse and the computer simulation. In order to simulate the nature of the laser ionization mechanism the clustering was switched off. Figure 2a shows the response of Boie's amplifier [3] to an impulse charge. This shape was used in the program to simulate the amplifier's contribution to the final pulse width. Since no zero-pole filter [3] was used behind the amplifier, we left the full $1/t$ response due to positive ion motion [5] in the convolution. The disagreement in the tail region can be explained by a saturation effect, since the chamber operated at a gain of the order of $\sim 10^5$. We have made similar comparisons in a larger chamber operating at normal pressure with and without zero-pole filters and found very good agreement.

The analysis of the resolution in the micro-jet chamber was done in the following way. We selected points by fitting a straight line to three points with a $\pm 3\sigma$ cut. Since we used only three points, we quote the resolution based on the measurement of a quantity $\Delta = (\frac{T1+T3}{2} - T2)$. Figure 4 shows the measured distribution of this quantity in a $10GeV$ electron beam. We fit a Gaussian curve to these distributions and determine $\sigma_\Delta$. The final quoted quantity is $\sigma = (\frac{2}{3})^{1/2} \sigma_\Delta v_D$. Figure 5 shows the measured dependence of $\sigma$ on the impact parameter in a $10GeV$ $e^+$ beam. Figure 6 indicates that a further improvement in the resolution is possible, however, we have to add a good quality second stage amplification. With the nitrogen laser the measured resolution was slightly worse, presumably due to a presence of slightly larger noise from the spark gap

– see fig. 2b. The achieved resolution was $\sim 24\mu m$ in $90\% Ar + 10\% C_4H_{10}$ for an ionization yield comparable to that of $10GeV$ $e^+$ beam.

The calibration using an $F_e^{55}$ source and $90\% Ar + 9\% CO_2 + 1\% CH_4$ gas indicates several useful dependencies, namely $\Delta Gain/\Delta V_{SIDE} \simeq$ a factor of $6/1kV$ at $6atm$, $\Delta V_{SIDE}/\Delta p \simeq 0.5kV/atm$ to keep a constant gain, $\Delta Peak\ signal/\Delta p \simeq$ a factor of $2/atm$ at $V_{SIDE} = -7kV$.

Finally, we measured an average drift pulse shape in a $10GeV$ electron beam and concluded that the expected double track resolution in this chamber should be $\sim 600-800\mu m$ with simple time over threshold digital method – see fig. 7.

Having gained confidence in the drift program, we have used it to predict the pulse shapes for particles by creating an ionization in clusters – see fig. 8. The detailed analysis of these pulse shapes indicates that multiple threshold timing with the realistic pulses would improve the timing resolution compared to leading edge timing, provided that the drift pulses are not limited by the amplifier or by wire saturation. However, the improvement is only $\sim 20\%$ and it might not be worth the additional cost. We find that centroid peak timing from a parabolic fit to the peak to be twice worse than leading edge timing. We were not able to find a practical algorithm which would achieve equally good results as the best resolution obtained assuming infinitely fast electronics capable of digitizing every arriving electron and making a centroid average over the first $\sim 1ns$. Similar conclusions can be drawn for cells, such as the new *MARKII, SLD* [4], et cetera. Generally, one expects dependency of such conclusions on the pressure, drift distance and the magnetic field value, et cetera.

## 3. CONCLUSION

We believe that it is possible to achieve $\sim 20-25\mu m$ resolution in practical systems with the micro-jet chamber concept, provided that we treat the chamber as we treat the *TOF* systems. This limits the size of the system to 200-300 wires.

## ACKNOWLEDGEMENTS

I would like to thank Dr. L. Keller for support during this project. I would like to thank my summer student, L. Roberts, for software help in developing the drift program.

The help of R. Gearhart and the accelerator operations staff during the beam test is appreciated.

## APPENDIX A

(Brief description of the drift program.)

There have been other attempts to simulate drift pulses [5,6]; however, neither work was complete. We started from an electrostatic program [7], which calculates a two-dimensional electrostatic field given the wire radii and potentials. The following are the main points of our analysis:

1. We create a segment of a track with clustering according to Piuz and Lapique [8]. Each electron within the cluster is drifted independently.
2. The drift velocity and diffusion is determined at each point according to the $\frac{E}{p}$ and the magnetic field $B$.
3. The diffusion is simulated by radomizing each step, both in the longitudinal and transverse directions. The sigmas of the diffusions are taken from the measurement by parameterizing the longitudinal and transverse diffusion as a function of $\frac{E}{p}$. In the absence of such measurements we use $\sigma_x = \sigma_x^0(\frac{\epsilon_K x}{E})^{1/2}$, $\sigma_L \simeq \frac{1}{2}\sigma_x - \sigma_x$, where $x$ is the step length, $\epsilon_K = (\frac{E}{p})^\alpha$ for $\frac{E}{p} > const.$, $\epsilon_K = (const.)^\alpha$ for $\frac{E}{p} < const.$, $E$ is the electric field, $p$ is the pressure and $\sigma_x^0$ is the normalization constant. (We use $\sigma_x^0 = 380\mu m$ normalized at $1kV/cm$, $1atm$ and $1cm$ of drift; $\alpha = 1.3$ and $const. = 0.02kV/cm$ for $90\,\%\,Ar + 10\,\%\,C_4H_{10}$).
4. The avalanche fluctuation is simulated by assigning a weight $x$ to each electron according to the following weighting function, $A(x) = const.\ x\ e^{-1.5x}$ [9].
5. The effect of the positive ions is simulated by convoluting the drift time distribution with a function $i(t) \alpha \frac{1}{1+t/t_0}$ [5], where $t_0 = r_a/2\mu E_a \sim 0.1 - 0.2ns$ for $r_a = 3.9\mu m, \mu \sim 1.5cm^2\ V^{-1}\ sec^{-1}$, $E_a \simeq 940kV/cm$ in the micro-jet chamber and $90\,\%\,Ar + 10\,\%\,C_4H_{10}$ gas.
6. The effect of the electronics is simulated semi-empirically by measuring an amplifier's response to a step charge and convoluting this function with the rest of the distribution. At this point we include the effect of filters and noise.

**Table 1**

| Gas | $V_{SIDE}$ (kV) | p (atm) | E/p (kV/cm atm) | $v_D$ (cm/μsec) | σ (μm) in 10 GeV $e^+$ beam[4) |
|---|---|---|---|---|---|
| 90% Ar + 10% $C_4H_{10}$ [1) | -7.0 | 6.1 | 2.39 | 3.28 | 22 |
| 90% Ar + 10% $C_4H_{10}$ | -6.5 | 6.1 | 2.23 | 3.29 | 25 |
| 90% Ar + 10% $C_4H_{10}$ | -6.0 | 6.1 | 2.05 | 3.34 | 31 |
| 75% $C_3H_8$ + 25% $C_2H_4$ [13] [2) | -10.0 | 4.1 | 5.15 | 5.03 | 29 |
| 90% Ar + 9% $CO_2$ + 1% $CH_4$ | -7.4 | 6.1 | 2.52 | 4.31 | 37 |
| $[(CH_3)_2\,O]$ [11] [3) | -8.0 | 3.0 | 5.43 | 3.4 | -- |

**($V_{GUARD} = 0$ in all above runs.)**

Notes:

1. We are planning to add ∼ 10 × amplification stage to reduce the gain in the chamber.
2. Added ∼ 10 × amplification stage to Boie's amplifier.
3. Added ∼ 100 × amplification stage to Boie's amplifier.
4. $FWHM = 0.9mm$, impact parameter $= 2mm$.

## REFERENCES


1. J. Va'vra, SLC note 60.
2. J. Va'vra, IEEE Trans. Nucl. Sci. (October 1982) or SLAC-PUB-2984.
3. R. A. Boie, A. T. Hrisoho and P. Rehak, Nucl. Instr. and Meth. 192 (1982) 365.
4. SLD proposal for the SLC experiment at SLAC.
5. G. R. Ricker and J. J. Gomes, The Rev. of Sci. Instr. 40 (1969) 227.
6. K. Bunnell, MARK III program (1979), unpublished.
7. D. Miller and R. H. Schindler, MARK II program (1978), unpublished.
8. F. Lapique and F. Piuz, Nucl. Instr. and Meth. 175 (1980) 297.
9. S. C. Curran, A. L. Cocroft and J. Angus, Phil. Mag. 40 (1949) 929.
10. A. H. Walenta et al., Proc. of Int. Conf., SLAC-Report 250, 1982.
11. F. Villa, SLAC-PUB-3037.
12. J. Va'vra and L. Roberts, to be published.
13. W. Farr et al., Nucl. Instr. and Meth., 154 (1978) 175.

FIGURE CAPTIONS

1. The micro-jet chamber prototype.

2. a) Response of the Boie's amplifier to an impulse charge of $2.3 \times 10^5$ electrons ($50\Omega$). b) The laser induced drift pulse and the diode pulse at $7.2atm$, $V_{SIDE} = -6kV$, $V_{GUARD} = -1kV$ and $90\,\%\,Ar + 9\,\%\,CO_2 + 1\,\%\,CH_4$.

3. Comparison of measured drift pulse in the laser beam and the computer simulation.

4. Experimental results in $10GeV$ electron beam and $90\,\%\,Ar + 10\,\%\,C_4H_{10}$ gas at $6.1atm$, $V_{SIDE} = -7.0kV$, $V_{GUARD} = 0\ V$.

5. Final resolution as a function of the impact parameter in $90\,\%\,Ar + 10\,\%\,C_4H_{10}$, $6.1atm$, $V_{SIDE} = -7kV$, $V_{GUARD} = 0\ V$.

6. Resolution as a function of $V_{SIDE}$ voltage.

7. Average drift pulse shapes in the micro-jet chamber measured in $10GeV$ $e^+$ beam.

8. The computer simulation of the drift pulses caused by particles in the micro-jet chamber ($V_{SIDE} = -7kV$, $V_{GUARD} = 0\ V$).

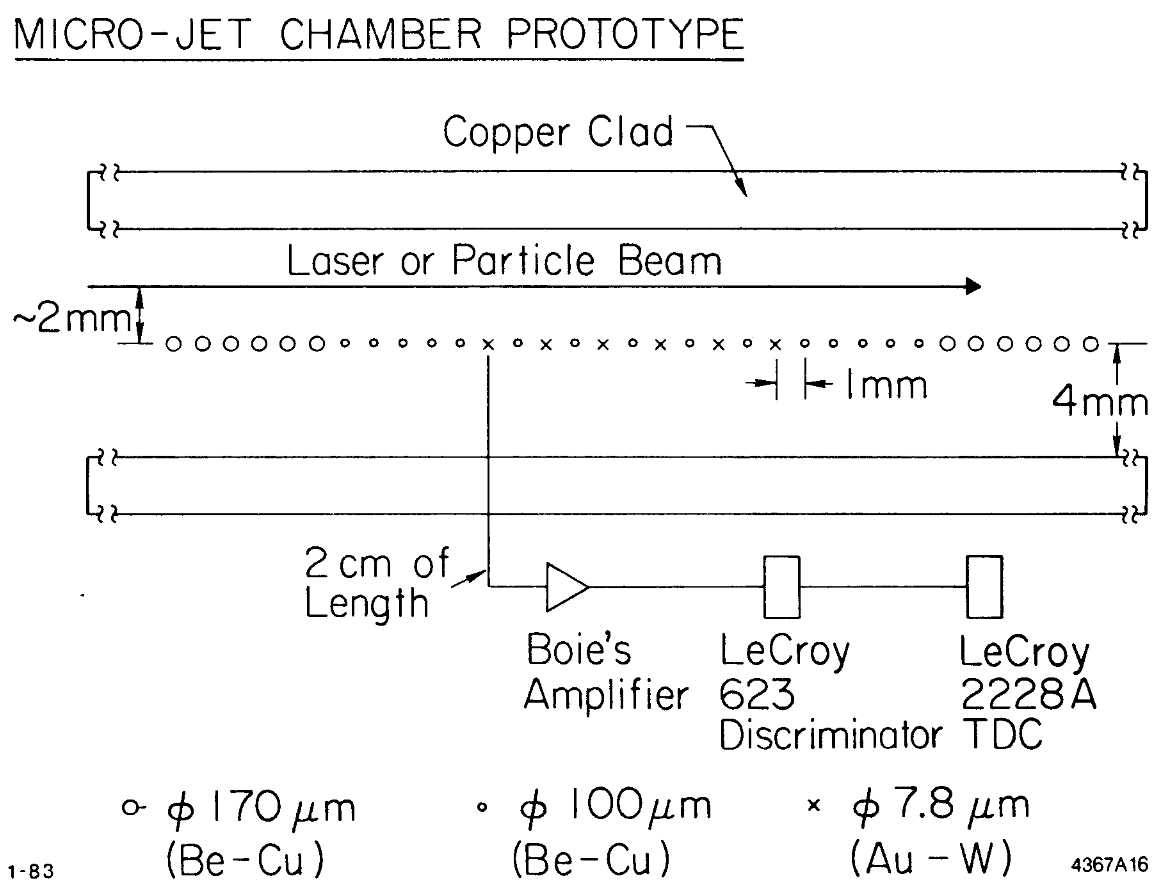
MICRO-JET CHAMBER PROTOTYPE
Copper Clad
Laser or Particle Beam
~2mm
1mm
4mm
2 cm of Length
Boie's Amplifier
LeCroy 623 Discriminator
LeCroy 2228A TDC
ϕ 170 μm (Be-Cu)
ϕ 100μm (Be-Cu)
ϕ 7.8 μm (Au-W)
1-83
4367A16

Fig. 1

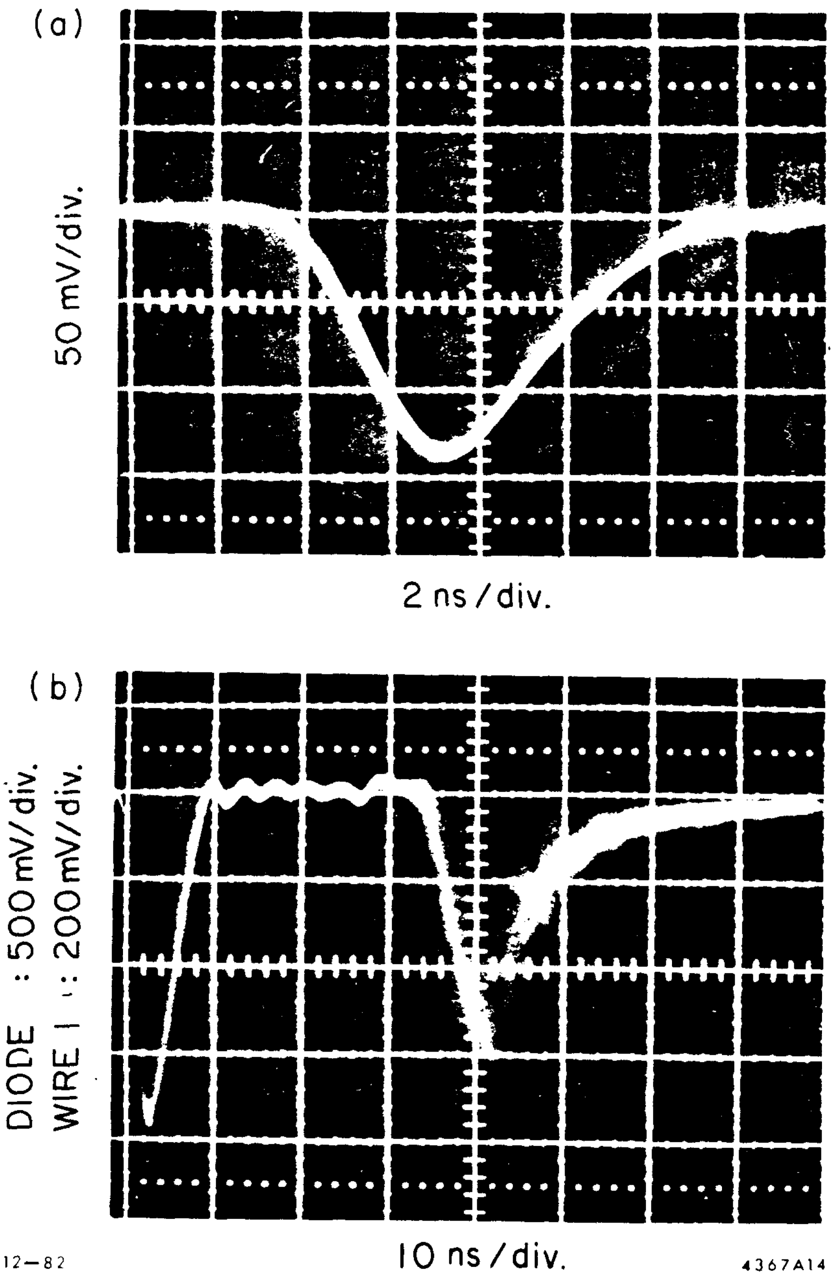
(a)
50 mV/div.
2 ns/div.
(b)
DIODE : 500 mV/div.
WIRE 1 : 200 mV/div.
10 ns/div.
12-82
4367A14

Fig. 2

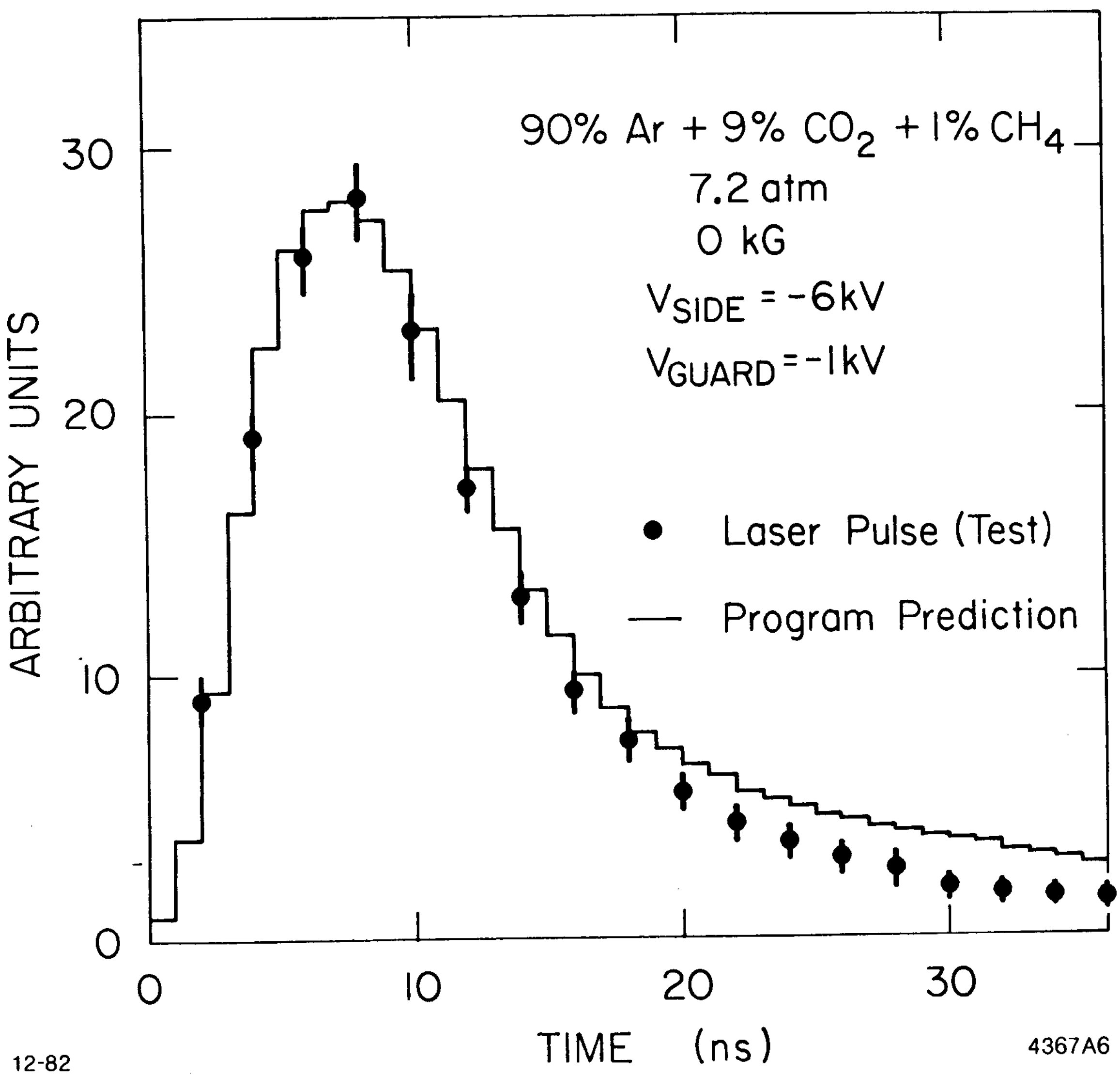

$90\%$ Ar + $9\%$ $CO_2$ + $1\%$ $CH_4$
7.2 atm
0 kG
$V_{SIDE}$ = −6kV
$V_{GUARD}$ = −1kV
Laser Pulse (Test)
Program Prediction
ARBITRARY UNITS
0
10
20
30
TIME (ns)
12-82
4367A6


Fig. 3

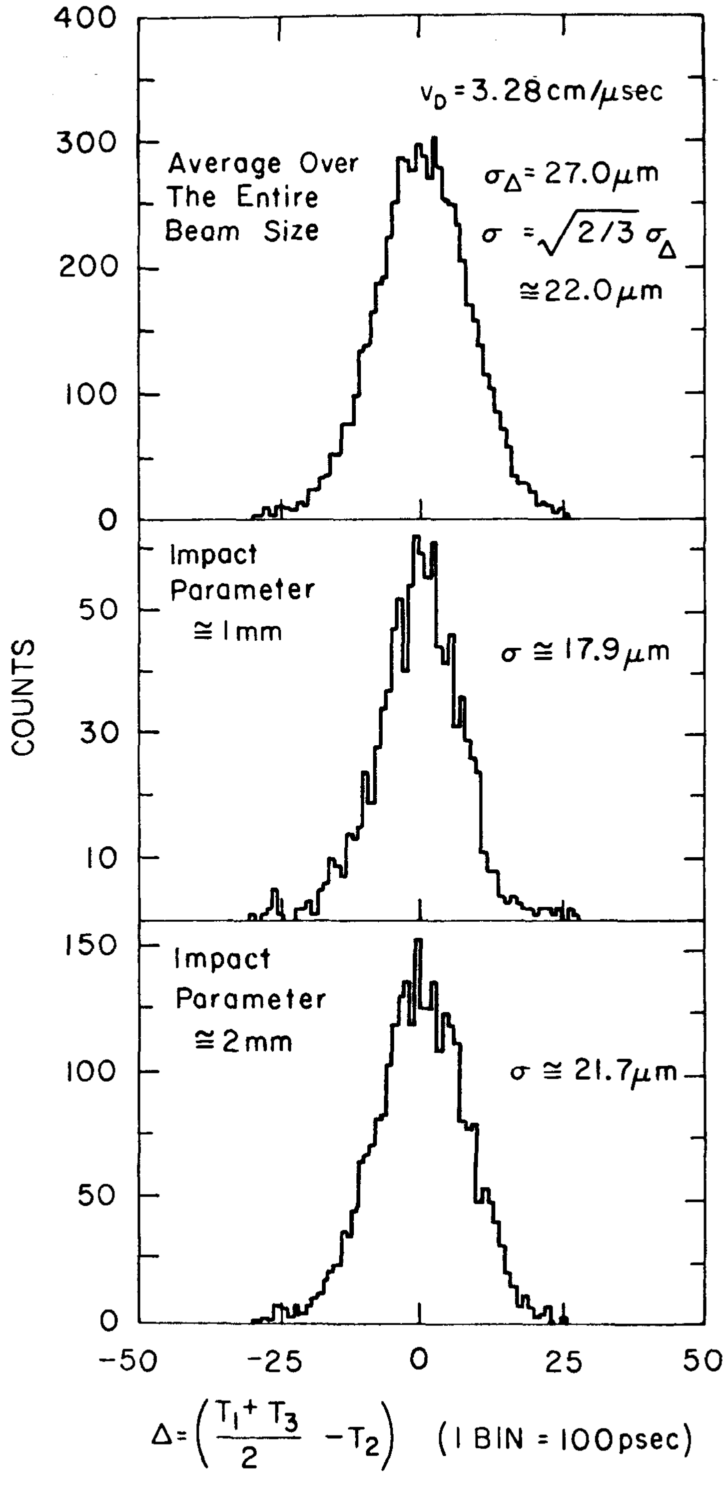


1–83 4367A19

Fig. 4

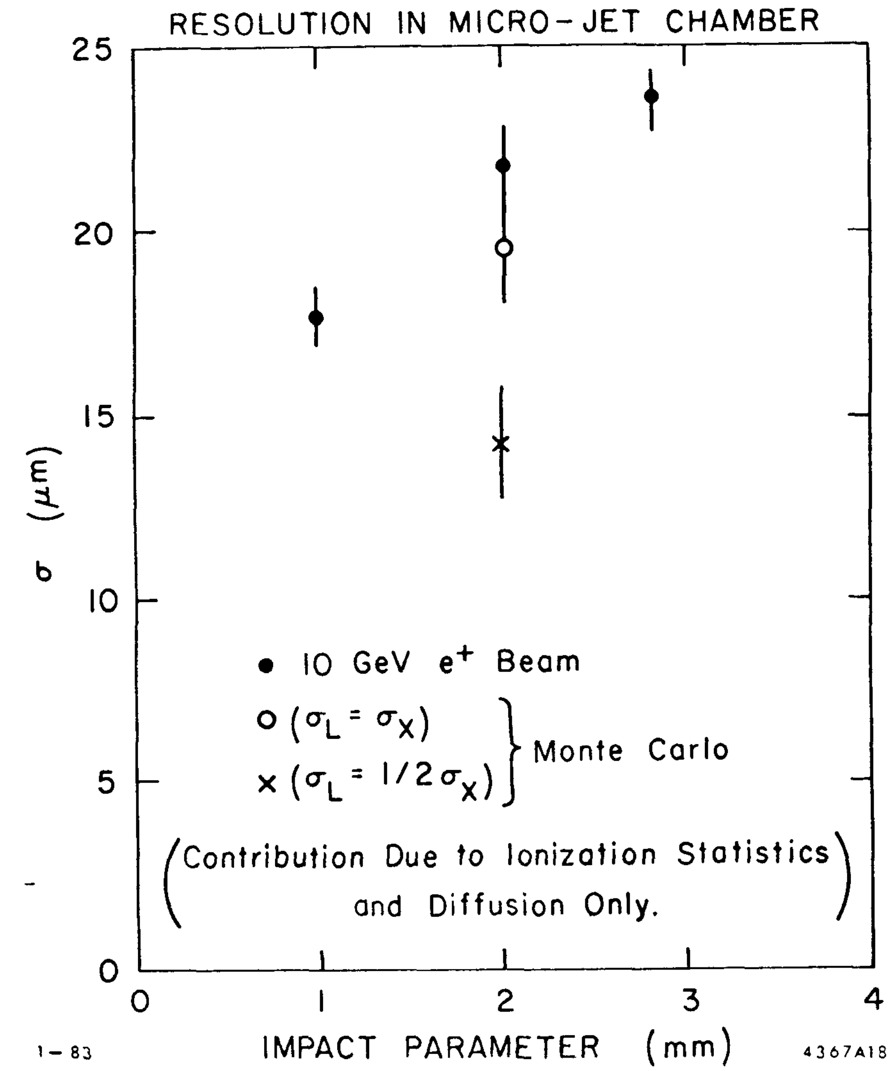
RESOLUTION IN MICRO-JET CHAMBER
25
20
15
10
5
0
σ (μm)
● 10 GeV e+ Beam
o (σL = σX)
× (σL = 1/2 σX)
Monte Carlo
(Contribution Due to Ionization Statistics and Diffusion Only.)
0
1
2
3
4
IMPACT PARAMETER (mm)
1-83
4367A18

Fig. 5

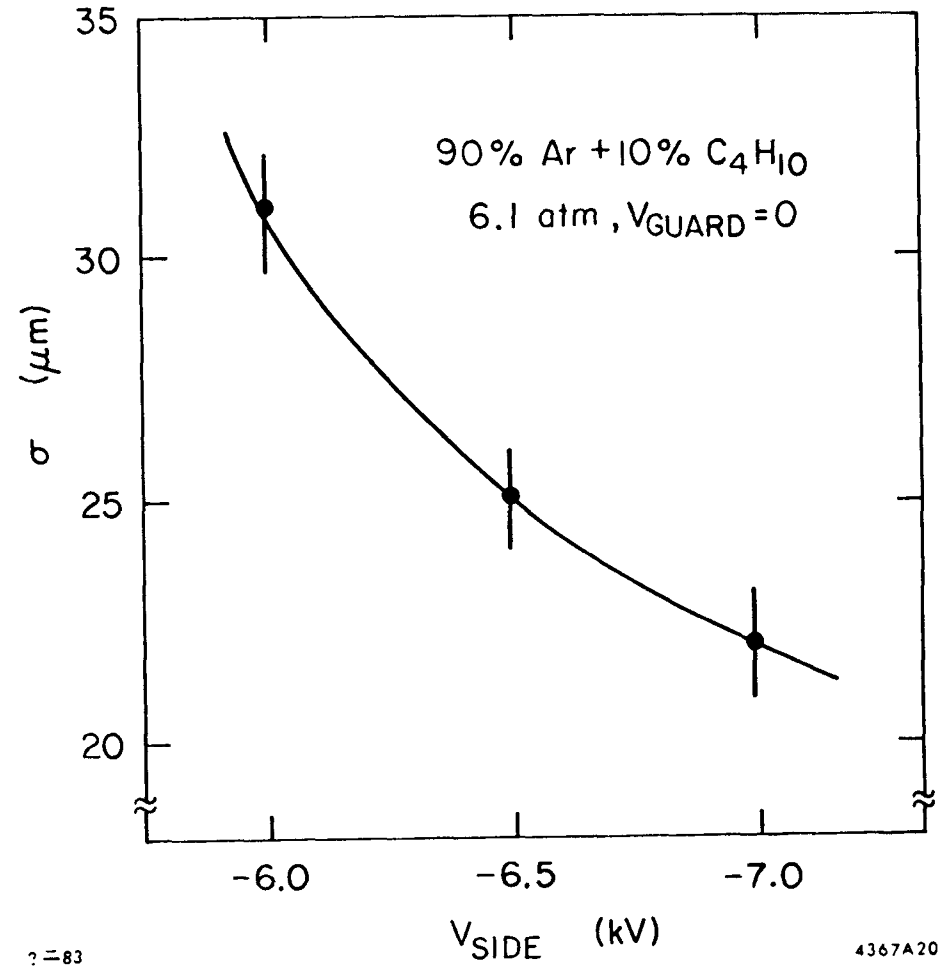
35
30
25
20
σ (μm)
90% Ar + 10% C4H10
6.1 atm , VGUARD = 0
-6.0
-6.5
-7.0
VSIDE (kV)
? =83
4367A20

Fig. 6

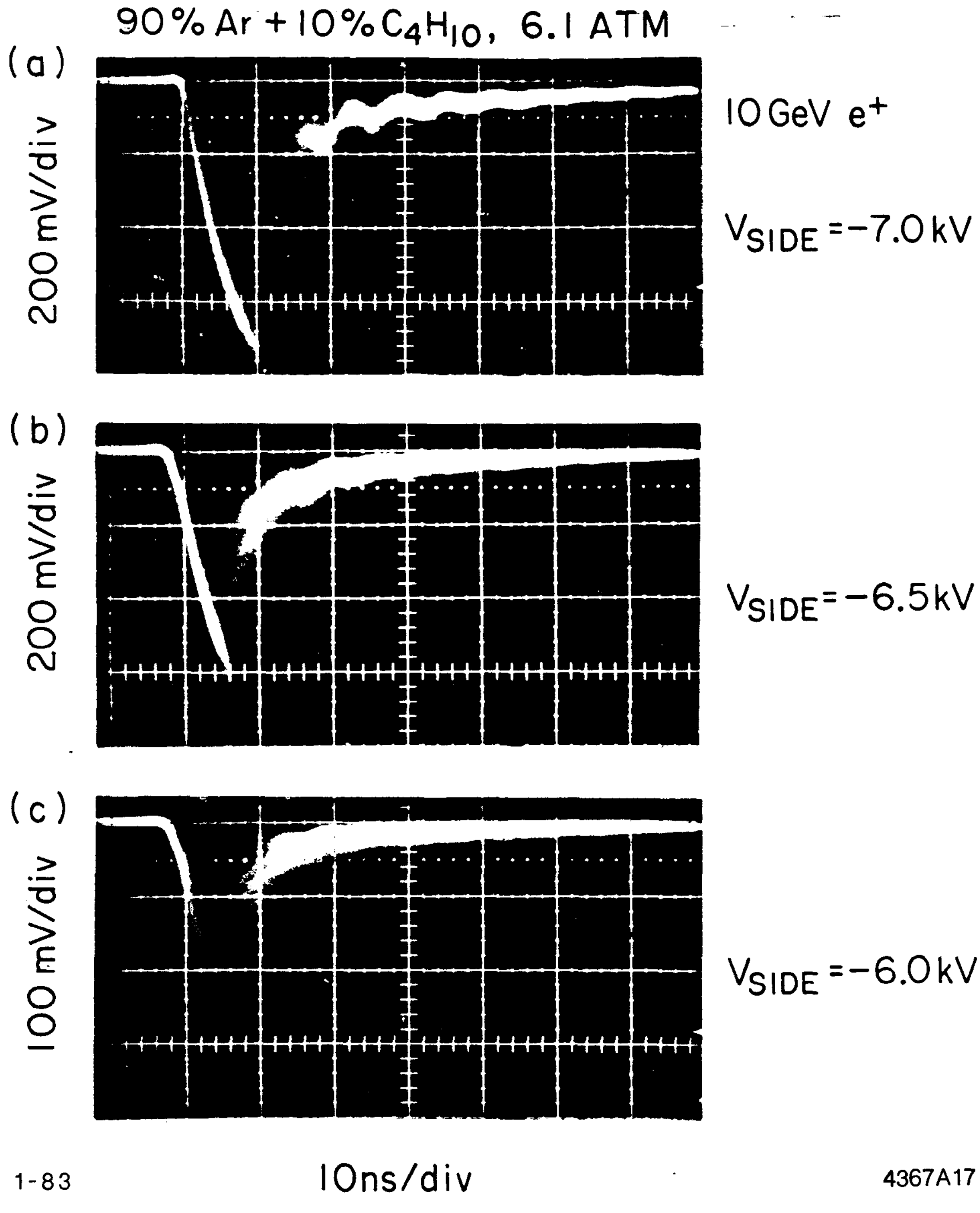
90% Ar + 10% $C_4H_{10}$, 6.1 ATM
(a)
200 mV/div
10 GeV $e^+$
$V_{SIDE}$ = −7.0 kV
(b)
200 mV/div
$V_{SIDE}$ = −6.5 kV
(c)
100 mV/div
$V_{SIDE}$ = −6.0 kV
1-83
10 ns/div
4367A17

Fig. 7

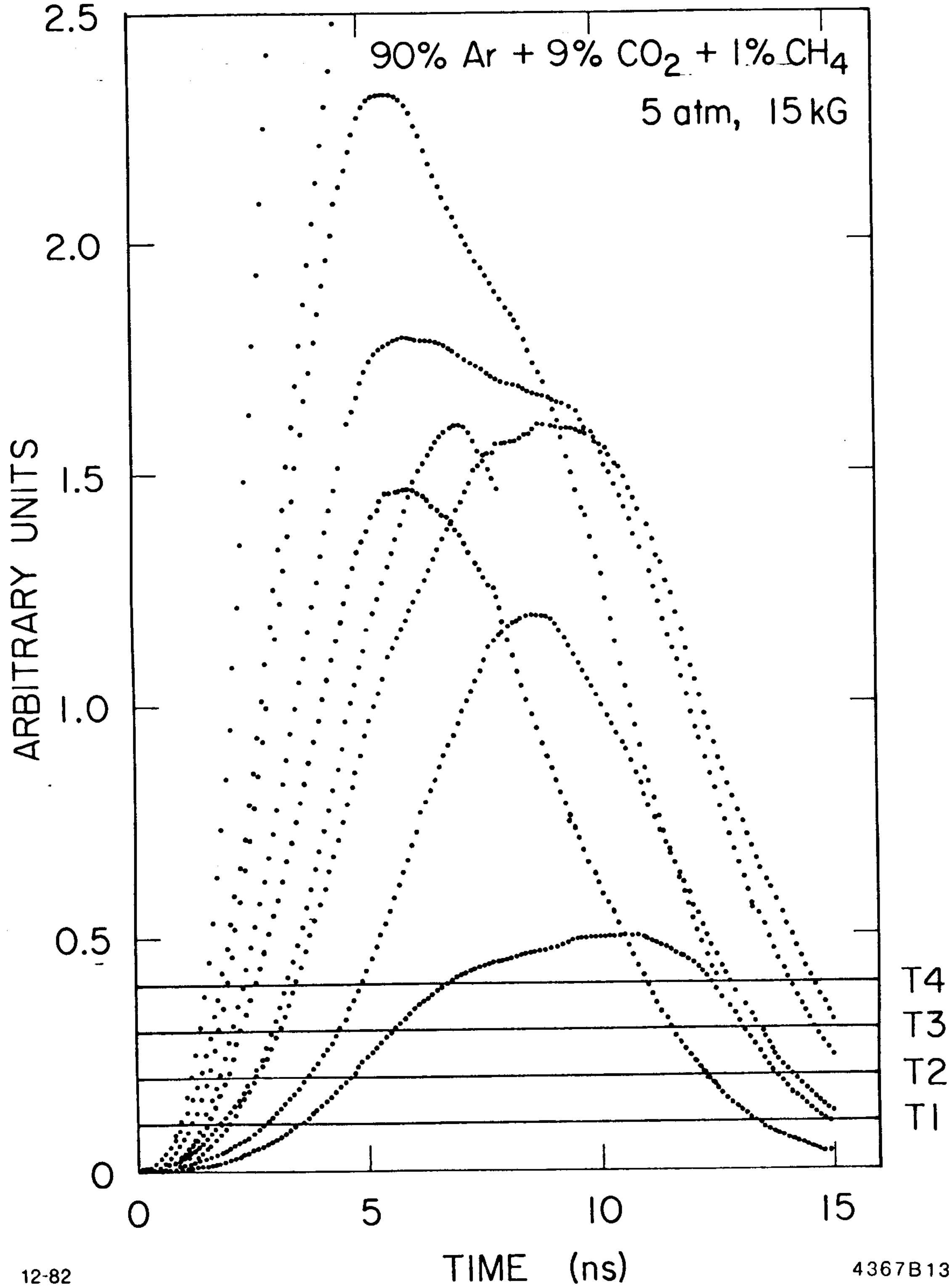

90% Ar + 9% $CO_2$ + 1% $CH_4$
5 atm, 15 kG
2.5
2.0
1.5
1.0
0.5
0
ARBITRARY UNITS
T4
T3
T2
T1
0
5
10
15
TIME (ns)
12-82
4367B13


Fig. 8